RsrR: a novel redox sensitive Rrf2 family transcription factor in *Streptomyces venezuelae*

John T. Munnoch[1], M[a] Teresa Pellicer Martinez[2], Dimitri A. Svistunenko[3], Jason C. Crack[2], Nick E. Le Brun[2#] and Matthew I. Hutchings[1#]

[1]School of Biological Sciences, University of East Anglia, Norwich, Norwich Research Park, NR4 7TJ

[2]Centre for Molecular and Structural Biochemistry, School of Chemistry, University of East Anglia, Norwich, Norwich Research Park, NR4 7TJ

[3]School of Biological Sciences, University of Essex, Wivenhoe Park, Colchester CO4 3SQ

Running Head: RsrR is a novel redox sensor in *S. venezualae*.

[#]Address correspondence to: n.le-brun@uea.ac.uk; m.hutchings@uea.ac.uk

Abstract length: 225 words.

Text length: 6870 words.

Abstract. Members of the Rrf2 superfamily of transcription factors are widespread in bacteria but their biological functions are largely unknown. The few that have been characterised in detail sense nitric oxide (NsrR), iron limitation (RirA), cysteine availability (CymR) and the iron sulphur (Fe-S) cluster status of the cell (IscR). Here we combine ChIP-seq, ChIP-exo and dRNA-seq with *in vitro* biochemistry to characterise a new member of the Rrf2 family in the model organism *Streptomyces venezuelae*. We show that Sven6563 has a redox active [2Fe-2S] cluster and that the switch from oxidized to reduced cluster switches off DNA binding activity. We have named the protein RsrR for Redox sensitive response Regulator. Binding site positions at target promoters combined with expression data suggest RsrR acts primarily as a repressor, like other Rrf2 proteins. ChIP shows that RsrR can bind to class 1 target promoters containing an 11-3-11bp inverted repeat motif and class 2 target promoters containing a single 11 bp motif. All 630 ChIP-exo peaks contain at least one motif, suggesting a global role for RsrR. However, the strongest targets are class 1 and include NAD(P)+ dependent enzymes, NAD(P)+ biosynthetic enzymes, the NADH and NADPH dehydrogenases and a putative NAD(P)+ binding regulator that is divergently transcribed from *rsrR*. Thus, our data suggest RsrR senses redox changes in the cell and has a primary role in regulating NAD(P)H metabolism.

Importance. Redox stress, Fe-S proteins, Rrf2 regulators and actinomycetes.

Introduction. Filamentous *Streptomyces* bacteria produce bioactive secondary metabolites that account for more than half of all known antibiotics as well as anticancer, anti-helminthic and immunosuppressant drugs (1, 2). More than 600 *Streptomyces* species are known and each encodes between 10 and 50 secondary metabolites but only 25% of these compounds are produced *in vitro* so there is huge potential for the discovery of new natural products from *Streptomyces* and their close relatives. This is revitalizing research into these bacteria and *Streptomyces venezuelae* has recently emerged as a new model for studying their complex life cycle, in part because of its unusual ability to sporulate to near completion when grown in submerged liquid culture. This means the different tissue types involved in the progression to sporulation can be easily separated and used for tissue specific analyses such as RNA and ChIP-seq (3, 4). *Streptomyces* species are complex bacteria that grow like fungi, forming a branching, feeding substrate mycelium in the soil that differentiates upon nutrient stress into reproductive aerial hyphae that undergo cell division to form spores (5). Differentiation is closely linked to the production of antibiotics which are presumed to offer a competitive advantage when nutrients become scarce in the soil.

Streptomyces bacteria are well adapted for life in the complex soil environment with more than a quarter of their ~9 Mbp genomes encoding one and two-component signaling pathways that allow them to rapidly sense and respond to changes in their environment (6). They are facultative aerobes and have multiple systems for dealing with redox, oxidative and nitrosative stress. Most species can survive for long periods in the absence of O_2, most likely by respiring nitrate, but the molecular details are not known (7). They deal effectively with nitric oxide (NO) generated either endogenously through nitrate respiration (7) or in some cases from dedicated bacterial NO synthase (bNOS) enzymes (8) or by other NO generating organisms in the soil (9). We recently characterised NsrR, which is the major bacterial NO stress sensor in *Streptomyces coelicolor* (ScNsrR). NsrR is a dimeric Rrf2 family protein with

one [4Fe-4S] cluster per monomer that reacts rapidly with up to eight molecules of NO (10, 11). Nitrosylation of the Fe-S cluster results in derepression of the *nsrR*, *hmpA1* and *hmpA2* genes (11), which results in transient expression of HmpA NO dioxygenase enzymes that convert NO to nitrate (12–14). The Rrf2 superfamily of bacterial transcription factors is still relatively poorly characterised, but many have C-terminal cysteine residues that are known or predicted to coordinate Fe-S clusters. Other characterised Rrf2 proteins include RirA which senses iron limitation most likely through an Fe-S cluster (15) and IscR which senses the Fe-S cluster status of the cell (16).

In this work we report the characterisation of the *S. venezuelae* protein Sven6563 and show that it is a novel member of the Rrf2 superfamily. We have named this protein RsrR for Redox sensitive response Regulator. Although it is annotated as an NsrR homologue it shares only 27% identity with ScNsrR and is not genetically linked to an *hmpA* gene (Fig. S1 and S2). We purified the RsrR protein under anaerobic conditions and found that is a dimer with each monomer containing a reduced [2Fe-2S] cluster that is rapidly oxidized but not destroyed by oxygen. In fact we show the cluster can switch easily between oxidized and reduced states and provide evidence that this switch controls its DNA binding activity. Chromatin immunoprecipitation followed by sequencing (ChIP-seq) analysis of RsrR in *S. venezuelae* combined with dRNA-seq and EMSA studies allowed us to define the RsrR regulon and binding sites and determine that it acts primarily as a transcriptional repressor. Little fluctuation in the expression pattern of target genes is observed between wild-type and *ΔrsrR* strains which we hypothesis is due to additional levels of regulation, primarily by a divergent regulator, NmrA, whose expression is controlled by RsrR. Class 1 RsrR targets contain at least one 11-3-11bp inverted repeat while class 2 targets contain only half sites, with a single 11bp motif. Class 1 targets are most strongly enriched *in vivo* but there is little difference in binding affinity *in vitro* suggesting additional nucleotides may enhance binding

to class 2 sites that are not identified using MEME. This is supported by the fact that RsrR binds weakly to artificial half sites *in vitro*. Class 1 target genes include NAD(P) dependent oxidoreductases and the NADH and NADPH dehydrogenase operons consistent with a primary role for RsrR in regulating NAD(P)H metabolism in response to redox changes in the cell.

Results

RsrR regulates genes involved in NAD(P)H metabolism. To investigate RsrR function in *S. venezuelae* we decided to first identify target genes for RsrR in *S. venezuelae*. We constructed an *S. venezuelae* Δ*rsrR* mutant that expresses an N-terminally 3xFlag-tagged RsrR protein and performed ChIP-seq against this strain and wild-type *S. venezuelae* (ChIP-Seq accession number - TBC). The sequencing reads from the wild-type (control) sample were subtracted from the experimental sample before ChIP peaks were called (Fig. 1A). With no defined cut-off or arbitrary cut-offs of ≥200 reads or ≥500 sequencing reads per peak we identified >2700, >600 and 119 enriched target sequences, respectively (Supplementary File S1). A subset of the 119 targets can be found in Table 1. Working with the shortlist of 119 targets we confirmed the peaks by visual inspection of the data using Integrated Genome Browser (17). Fourteen of the ChIP peaks are in intergenic regions between divergent genes giving a total of 133 possible targets (Table S3). The core MEME suite tool, MEME (18) was used to search for a consensus RsrR binding site in all 119 sequences and identified a single conserved motif present in all 126 sequences (Fig. 1B and Supplementary File S4). In 14 of these 119 peaks a motif is present corresponding to an inverted 11-3-11bp repeat, which is characteristic of full-length Rrf2 binding sites and we called these class 1 targets (Fig. 1C, Table 1 and Supplementary File S5). Previous studies of *E. coli* NsrR have suggested that target genes with full 11bp inverted repeat binding sites are most strongly repressed and

115 therefore most physiologically relevant, thus perhaps giving clues about the primary function
116 of RsrR. Two of the class 1 sites are between divergent genes (*sven3827/8 and sven6562/3* –
117 the *rsrR* peak). The 107 bp intergenic region between *sven6562* and *rsrR*, contains two
118 putative class 1 RsrR binding sites separated by a single base pair. *sven6562* encodes a LysR
119 family regulator with an NmrA-type ligand binding domain predicted to sense redox poise by
120 binding NAD(P)+ but not NAD(P)H (19). From hereon we refer to *sven6562* as *nmrA*. The
121 positions of the two RsrR binding sites relative to the transcript start sites (TSS) of *sven6562*
122 and *rsrR* suggests that RsrR represses transcription of both genes by blocking the RNA
123 polymerase binding site. Other class 1 targets include the *nuo* (NADH dehydrogenase)
124 operon *sven4265-78* (*nuoA-N*) which contains an internal class 1 RsrR site (upstream of
125 *sven4272*, *nuoH*), the putative NADP+ dependent dehydrogenase Sven1847 and the quinone
126 oxidoreductase Sven5174 which converts quinone and NAD(P)H to hydroquinone and
127 NAD(P)+ (Table 1). Based on this data we suggest RsrR plays a primary role in regulating
128 NAD(P)H metabolism and possibly senses redox poise in the cell. Intriguingly, however,
129 dRNA-seq (expression data for the regulon is available in File S1.5 and TSS data in S3.6-9)
130 (dRNA-seq accession number - TBC) suggests only a single class 1 targets is induced in an
131 *rsrR* mutant and that is the divergent gene *nmrA*. This is probably because the other genes are
132 subject to more complex regulation from multiple transcription factors. The remaining 105
133 genes on the RsrR shortlist were classified as class 2 targets because they have single copies
134 of the class 2 motif, which we call half sites (Fig. 1B). Half sites have been observed for
135 other Rrf2 proteins including *E. coli* NsrR and these half-site promoters are subject to much
136 weaker repression and their physiological relevance is unclear (20–22).
137
138 **Purified RsrR contains a redox active [2Fe-2S] cluster.** RsrR contains three C-terminal
139 cysteine residues which is characteristic of Rrf2 proteins that ligate Fe-S clusters. To

investigate the cofactor and DNA binding activity of RsrR we over-expressed the *rsrR* gene in *E. coli* and purified the protein under strictly anaerobic conditions. Upon purification, the fractions containing RsrR were pink in colour but rapidly turned brown when exposed to O_2, suggesting the presence of a redox-active cofactor. The UV-visible absorbance spectrum of the as isolated protein, Fig. 2A, revealed broad weak bands in the 300- 640 nm region. Following exposure to O_2, the spectrum changed significantly, with a more intense absorbance band at 460 nm and a pronounced shoulder feature at 330 nm (Fig. 2A). The form of the reduced and oxidized spectra are similar to those previously reported for [2Fe-2S] clusters that are coordinated by three Cys residues and one His (23, 24). The anaerobic addition of dithionite to the previously air-exposed sample (at a 1:1 ratio with [2Fe-2S] cluster as determined by iron content) resulted in a spectrum very similar to that of the as isolated protein (Fig. 2A), demonstrating that the cofactor undergoes redox cycling.

Because the electronic transitions of iron-sulfur clusters become optically active as a result of the fold of the protein in which they are bound, CD spectra reflect the cluster environment (25). The near UV-visible CD spectrum of RsrR (Fig. 2B) for the as isolated protein contained three positive (+) features at 303, 385 and 473 nm and negative features at (-) 343 and 559 nm. When the protein was exposed to ambient O_2 for 30 min, significant changes in the CD spectrum were observed, with features at (+) 290, 365, 500, 600 nm and (-) 320, 450 and 534 nm (Fig. 2B). The CD spectra are similar to those reported for Rieske-type [2Fe-2S] clusters (23, 26, 27), which are coordinated by two Cys and two His residues. Anaerobic addition of dithionite (1 equivalent of [2Fe-2S] cluster) resulted in reduction back to the original form (Fig. 2B) consistent with the stability of the cofactor to redox cycling.

The absorbance data above indicates that the cofactor is in the reduced state as isolated. [2Fe-2S] clusters in their reduced state are paramagnetic (S = ½) and therefore should give rise to an EPR signal. The EPR spectrum for the as isolated protein contained

signals at g = 1.997, 1.919 and 1.867 (Fig. 2C). These g-values and the shape of the spectrum are characteristic of a $[2Fe\text{-}2S]^{1+}$ cluster. The addition of excess sodium dithionite to the as isolated protein did not cause any changes in the EPR spectrum (Fig. 2C) indicating that the cluster was fully reduced as isolated. Exposure of the as isolated protein to ambient O_2 resulted in an EPR-silent form, with only a small free radical signal typical for background spectra, consistent with the oxidation of the cluster to the $[2Fe\text{-}2S]^{2+}$ form (Fig. 2C), and the same result was obtained upon addition of the oxidant potassium ferricyanide (data not shown).

To further establish the cofactor that RsrR binds, native ESI-MS was employed. Here, a C-terminal His-tagged form of the protein was ionized in a volatile aqueous buffered solution that enabled it to remain folded with its cofactor bound. The deconvoluted mass spectrum contained several peaks in regions that corresponded to monomer and dimeric forms of the protein, (Fig. S6). In the monomer region (Fig. 3A), a peak was observed at 17,363 Da, which corresponds to the apo-protein (predicted mass 17363.99 Da), along with adduct peaks at +23 and +64 Da due to Na^+ (commonly observed in native mass spectra) and most likely two additional sulfurs (Cys residues readily pick up additional sulfurs as persulfides (28), respectively. A peak was also observed at +176 Da, corresponding to the protein containing a [2Fe-2S] cluster. As for the apo-protein, peaks corresponding to Na^+ and sulfur adducts of the cluster species were also observed (Fig. 3A). A significant peak was also detected at +120 Da which corresponds to a break down product of the [2Fe-2S] cluster (from which one iron is missing, FeS_2). In the dimer region, the signal to noise is significantly reduced but peaks are still clearly present (Fig. 3B). The peak at 34,726 Da corresponds to the RsrR homodimer (predicted mass 34727.98 Da), and the peak at +352 Da corresponds to the dimer with two [2Fe-2S] clusters. A peak at +176 Da is due to the dimer containing one [2Fe-2S] cluster. A range of cluster breakdown products similar to those

detected in the monomer region were also observed (Fig. 3B). Taken together, the data reported here demonstrate that RsrR contains a [2Fe-2S] cluster that can be reversibly cycled between oxidised (+2) and reduced (+1) states.

Cluster- and oxidation state dependent binding of RsrR to RsrR-regulated promoter DNA. To determine which form of RsrR is able to specifically bind DNA, EMSA experiments using a highly enriched ChIP target *sven1847/8*. Increasing ratios of [2Fe-2S] RsrR to DNA resulted in a clear shift in the mobility of the promoter DNA from unbound to bound, see Fig. 4A. Equivalent experiments with cluster-free (apo) RsrR did not result in a mobility shift, demonstrating that the cluster is required for the observed DNA-binding activity. These experiments were performed aerobically and so the [2Fe-2S] cofactor would have been in its oxidised state. To determine if oxidation state affects DNA binding activity, EMSA experiments were performed with $[2Fe\text{-}2S]^{2+}$ and $[2Fe\text{-}2S]^{1+}$ forms of RsrR. The oxidised cluster was generated by exposure to air and confirmed by UV-visible aborbance. The reduced cluster was obtained by reduction with sodium dithionite (confirmed by UV-visible absorbance) and the reduced state was maintained using EMSA running buffer containing an excess of dithionite. The resulting EMSAs, Fig. 4B and C, show that, in both cases, DNA-binding occurred but the oxidised form bound significantly more tightly. Tight binding could be restored to the reduced RsrR samples by allowing it to re-oxidise in air (data not shown). We cannot rule out that the apparent low affinity DNA binding observed for the reduced sample results from partial re-oxidation of the cluster during the electrophoretic experiment. Nevertheless, the conclusion is unaffected: oxidised, $[2Fe\text{-}2S]^{2+}$ RsrR is the high affinity DNA-binding form.

Oxidised [2Fe-2S] RsrR binds strongly to class 1 and 2 promoters *in vitro*. To further investigate the DNA binding activities of $[2Fe\text{-}2S]^{2+}$ RsrR EMSAs were performed on two class 2 promoters *sven0247* and *sven519* (Fig. 5A). Both class 2 promoters we tested were shifted by oxidized [2Fe-2S] RsrR thus showing that RsrR binds strongly to both full and half site (class 1 and 2) promoters. To further test the idea of full and half site binding, we constructed a series of mutated *nmrA-rsrR* promoter fragments carrying both natural class 1 sites (Fig. 5B), or artificial half sites (Fig. 5C). The results show that RsrR binds strongly to both full class 1 binding sites at the *nmrA-rsrR* promoters (Fig. 5B) but RsrR binds only weakly to artificial half sites (Fig. 5C). This suggests that although MEME only calls half sites in most of the RsrR target genes identified by ChIP-seq they must contain sufficient sequence information in the other half to enable strong binding.

Mapping RsrR binding sites using ChIP-exo and dRNA-seq. MEME analysis of the ChIP-seq data detected only 14 full sites out of the >600 target sites bound by RsrR in *S. venezuelae*. However, ChIP-Seq and EMSAs show that RsrR binds tightly to target promoters whether they contain predicted class 1 or class 2 sites. To gain more information about RsrR recognition sequences and the positions of these binding sites at target promoters we combined dRNA-seq, which maps the start sites of all expressed transcripts, with ChIP-exo, which uses Lambda exonuclease to trim excess DNA away from ChIP complexes leaving only the DNA which is actually bound and protected by RsrR (ChIP-exo accession number -TBC). For dRNA-seq, total RNA was prepared from cultures of wild type *S. venezuelae* grown for 16 hours and for the Δ*rsrR* mutant. ChIP-exo was performed on the Δ*rsrR* strain producing Flag-tagged RsrR at a single 16 hour time point. The targets identified using ChIP-exo matched the previously identified ChIP-seq targets, with 630 target genes. Howeevr, the ChIP-exo peaks are on average only ~50bp wide. MEME analysis using all 630

239 ChIP-exo sequences identified the same class 2 binding motif in every sequence. We
240 identified transcript start sites (TSS) for 261 of the 630 RsrR target genes using dRNA-seq
241 data from the 16h time point (File S3.10). Fig. 6 shows a graphical representation of the
242 class 1 targets that have clearly defined TSS, indicating the centre of the ChIP peak, the
243 associated TSS and any genes within the ~200 bp frame. Based on the RsrR binding site
244 position, transcription repression is most likely either by obstruction of RNA polymerase
245 binding or blockage of transcription elongation where they are inside the coding sequence.
246 This is consistent with a primary role for RsrR as a transcriptional repressor.
247
248 **Discussion.** In this work we have characterised a new member of the Rrf2 protein family,
249 which is mis-annotated as an NsrR homologue in the *S. venezuelae* genome. The purified
250 protein contains a [2Fe-2S] cluster, which is stable in the presence of O_2 and can be
251 reversibly cycled between reduced (+1) and oxidized (+2) states. The $[2Fe\text{-}2S]^{2+}$ form binds
252 strongly to both class 1 and class 2 bonding sequences *in vitro*, whereas the $[2Fe\text{-}2S]^{1+}$ form
253 exhibited, at best, significantly weaker binding and the apo form does not bind to DNA at all.
254 Given these observations and the stability of the Fe-S cluster to aerobic conditions, we
255 propose that the activity of RsrR is modulated by the oxidation state of its cluster, becoming
256 activated for DNA binding through oxidation and inactivated through reduction. Exposure to
257 O_2 is sufficient to cause oxidation, but other oxidants may also be important *in vivo*. The
258 properties of RsrR described here are reminiscent of an *E. coli* [2Fe-2S] cluster containing
259 transcription factor called SoxR, which controls the regulation of another regulator, SoxS,
260 through the oxidation state of its cluster (29). However, SoxR is a transcriptional activator
261 that switches on *soxS* transcription upon oxidation of the cluster to its $[2Fe\text{-}2S]^{2+}$ state (29).
262 ChIP-seq and ChIP-exo analysis show that RsrR binds to a large regulon of ~630
263 genes in *S. venezuelae* and approximately 2% of these contain obvious class 1 binding sites,

with an 11-3-11 bp inverted repeat. The fact that class 1 target genes are involved in either signal transduction and / or NAD(P)H metabolism also points to a link with redox poise and recycling of NAD(P)H to NAD(P). The >600 class 2 target genes likely bind to a full site sequence based on our EMSA results however 1 half of the site is less conserved resulting in MEME artificially reporting half site sequences. In addition to the genes involved directly in NADH/NAD(P)H metabolism, class 2 targets include 22 transcriptional regulators, genes involved in both primary and secondary metabolism, RNA/DNA replication and modification genes, transporters (mostly small molecule), proteases and a large number of genes with no known function. One of the most strongly induced target promoters in the Δ*rsrR* mutant is the divergent *nmrA* gene that encodes a LysR family regulator with an N terminal NAD(P)+ binding domain. NmrA proteins are thought to control redox poise in fungi by sensing the levels of NAD(P), which they can bind, and NAD(P)H, which they cannot (30). This is intriguing since RsrR presumably senses redox stress through reduction of its [2Fe-2S] cluster and this induces expression of NmrA which could sense redox poise via the ratio of NAD(P)/NAD(P)H and modulate expression of its own (unknown) target genes. It will be interesting to identify the overlap in target genes between the RsrR and NmrA gene regulons. The Δ*rsrR* mutant has no obvious phenotype and is no more sensitive to redox active compounds or oxidative stress that the wild-type (not shown). This is not surprising given the number of systems in *Streptomyces* bacteria that can deal with reactive oxygen species and redox stress including detoxifying enzymes: Catalases, peroxidases (31) and superoxide dismutases (32) and associated regulators such as OxyR (33), SigR (34), OhrR (35), Rex (19) and SoxR (36).

NmrA proteins are similar in function to the Rex protein in Gram-positive bacteria for which NAD+ and NADH compete for binding. NAD+ enhances the DNA binding activity of Rex and NADH switches it off (37). Intriguingly, Rex is well conserved in Gram-positive

bacteria but is missing from most actinomycetes, with the exception of *Streptomyces* species where it was first characterised (19). The reverse is true of NmrA and RsrR, which are both conserved (as back to back genes) in most filamentous actinomycetes but are missing from other Gram-positive bacteria, including most *Streptomyces* species. The majority of the RsrR regulon genes identified here must be subject to more complex regulation because they are not induced in the Δ*rsrR* background. For example, the *nuo* (NADH dehydrogenase) operon *sven_4265-78* (*nuoA-N*) contains an internal class 1 RsrR site (upstream of *sven_4272*, *nuoH*) but is not expressed in the Δ*rsrR* strain. Nuo is alsdo known to be repressed by Rex in *S. coelicolor* (19) and probably other streptomycetes. It will be interesting to further investigate the potential co-regulation of RsrR and NmrA target genes and to further elucidate the global network controlled by RsrR.

Materials and Methods

Bacterial strains, plasmids, oligonucleotides and growth conditions. Bacterial strains and plasmids are listed in Table S6 and oligonucleotides are listed in Table S7. For ChIP-seq experiments, *S. venezuelae* strains were grown at 30 ^{o}C in MYM liquid sporulation medium (38) made with 50% tap water and supplemented with 200µl trace element solution (39) per 100ml and adjusted to a final pH.of 7.3. Disruption of *rsrR* was carried out following the PCR-targeting method (40) as described previously described (41, 42). Primers JM0109 and JM0110 were used to PCR amplify the apramycin disruption cassette from pIJ773. Cosmid SV-5-F05 was used as the template cosmid. The disruption cosmid (pJM026) was checked by PCR using primers JM0111 and JM0112. Antibiotic marked, double crossover exconjugants, were identified as previously described and confirmed once more with JM0111 and JM0112.

The 3x Flag tag copy of *rsrR* was synthesized by genescript (sequence is available in

Supplementary File S6) and subcloned into pMS82 using HindIII/KpnI and confirmed by PCR using primers JM0113 and JM0114.

ChIP (chromatin immunoprecipitation) – seq and exo.

ChIP-Seq was carried out as previously described (43). A spore inoculum (~5-10 ul of $1x10^8$ spores) sufficient to reach an OD600 of 0.35 after 8 hours of growth was added to 35ml of MYM tap media in 250 ml flasks containing springs. Following growth to the chosen time point, the entire content of the flask was transferred to a 50 ml falcon tube for crosslinking, which was carried out by incubation at 30^{o}C for 30 mins with 1% final concentration of formaldehyde (v/v). Crosslinking was quenched by incubation at room temperature with glycine (final concentration of 125 mM). Mycelium was harvested by centrifugation 4000 rpm at 4^{o}C for 10 minutes and washed twice with ice cold PBS before transfer to a 2 ml centrifuge tube. Pellets were resuspended in 0.75 ml lysis buffer (10 mM Tris-HCl pH 8.0, 50 mM NaCl, 10 mg/ml lysozyme, 1x protease inhibitor-Roche1186170001) and incubate at 37C for 10-25 mins. Then 0.75 ml 1x IP buffer (100mM tris-HCl pH 8.0, 250 mM NaCl, 0.5% Triton x-100, 0.1% SDS, 1x protease inhibitor (Roche)) was added and samples mixed by pipetting up and down. Samples were sonicated 7x at 50Hz, 10 sec/cycle with a 1 min incubation on ice after each cycle. DNA fragmentation was checked by agarose gel electrophoresis following phenol extraction of 25 µl of the crude lysate mixed with 75 µl of TE buffer with 100-200 µl of phenol/chloroform. Contaminating RNA was removed with 2 µl RNase (1mg/ml) added to extracted DNA followed by an incubation for 30 min at 37°C. A smear of DNA from 200 to 1000 bp with the majority of DNA 200-400 bp should be visible. Crude lysate was centrifuged at 13,000 rpm for 15 minutes at 4°C to clear the sample of cell debris. M2 affinity beads (Sigma-Aldrich #A2220) were prepared by washing in ½IP buffer

following manufacturers instructions. The cleared lysate was incubated with 40 µl of washed M2 beads and incubated for 4 h at 4C in a vertical rotor. The lysate was removed and the beads pooled into one 1.5 microfuge tube and washed in 0.5 IP buffer. The beads were transferred to a fresh microfuge tube and washed a further 3 times removing as much buffer as possible without disturbing the beads. The DNA-protein complex was eluted from the beads with 100 µl elution buffer (50 mM Tris-HCl pH7.6, 10mM EDTA, 1% SDS) by incubating at 65°C overnight. Removing the ~100µl elution buffer, an extra 50 µl of elution buffer was added and further incubated at 65^{o}C for 5 min. To extract the DNA 150 µl eluate, 2 µl proteinase K (10 mg/ml) was added and incubated 1.5 hrs at 55^{o}C. To the reaction 150 µl phenol-chloroform was added. Samples were vortexed and centrifuged at full speed for 10 min. The aqueous layer was extracted and purified using the Qiaquick column from Qiagen with a final elution using 50 µl EB buffer (Qiagen). The concentration of samples were determined using Quant-iT™ PicoGreen ® dsDNA Reagent (Invitrogen) or equivalent kit or by nanodrop measurement.

DNA sequencing of ChIP-Seq samples was carried out by GATC. ChIP-exo following sonication of lysates was carried out by Peconic LLC (State College, PA) adding an additional exonuclease treatment to the process as previously described (44).

RNA-seq

Mycelium was harvested at experimentally appropriate time points and immediately transferred to 2 ml round bottom tubes, flash frozen in liquid N_2, stored at -80^{o}C or used immediately. All apparatus used was treated with RNaseZAP (Sigma) to remove RNases for a minimum of 1 hour before use. RNaseZAP treated mortar and pestles were used, the pestle being placed and cooled on a mixture of dry ice and liquid N_2 with liquid N_2 being poured into the bowl and over the mortar. Once the bowl had cooled the mycelium samples were

363 added directly to the liquid N_2 and thoroughly crushed using the mortar leaving a fine powder
364 of mycelium. Grindings were transferred to a pre-cooled 50 ml Falcon tube and stored on dry
365 ice. Directly to the tube, 2 ml of TRI reagent (Sigma) was added to the grindings and mixed.
366 Samples are then thawed while vortexing intermittently at room temperature for 5-10 minutes
367 until the solution cleared. To 1 ml of TRI reagent resuspension, 200 µl of chloroform was
368 added and vortexed for 15 seconds at room temperature then centrifuged for 10 minutes at
369 13,000 rpm. The upper, aqueous phase (clear colourless layer) was removed into a new 2 ml
370 tube. The remainder of the isolation protocol follows the RNeazy Mini Kit (Qiagen)
371 instructions carrying out both on and off column DNase treatments. On column treatments
372 were carried out following the first RW1 column wash. DNaseI (Qiagen) was added (10 µl
373 enzyme, 70 µl RDD buffer) to the column and stored at RT for 1 hour. The column was
374 washed again with RW1 then treated as described in the manufacturer's instructions. Once
375 eluted from the column, samples were treated using TURBO DNA-free Kit (Ambion)
376 following manufacturer's instructions to remove residual DNA contamination.
377 Data analysis was carried out as described in the ChIP-Seq/exo section for visualisation, as
378 well as expression profiling using CLC genomics workbench 8 and the TSSAR webservice
379 for dRNA transcription start site analysis (45). In addition a manual visual processing
380 approach was carried out for each.
381
382 **Purification of RsrR.**
383 5 L Luria-Bertani medium (10 × 500 mL) was inoculated with freshly transformed BL21
384 (DE3) *E. coli* containing a pGS-21a vector with the *prsrR-His* insert. 100 µg/mL ampicillin
385 and 20 µM ammonium ferric citrate were added and the cultures were grown at 37 °C, 200
386 rpm until $OD_{600\ nm}$ was 0.6-0.9. To facilitate *in vivo* iron-sulfur cluster formation, the flasks
387 were placed on ice for 18 min, then induced with 100 µM IPTG and incubated at 30 ºC and

105 rpm. After 50 min, the cultures were supplemented with 200 µM ammonium ferric citrate and 25 µM L-Methionine and incubated for a further 3.5 h at 30 ºC. The cells were harvested by centrifugation at 10000 × g for 15 min at 4 ºC. Unless otherwise stated, all subsequent purification steps were performed under anaerobic conditions inside an anaerobic cabinet (O_2 < 2 ppm). Cells pellets were resuspended in 70 mL of buffer A (50 mM TRIS, 50 mM $CaCl_2$, 5% (v/v) glycerol, pH 8) and placed in a 100 mL beaker. 30 mg/mL of lysozyme and 30 mg/mL of PMSF were added and the cell suspension thoroughly homogenized by syringe, removed from the anaerobic cabinet, sonicated twice while on ice, and returned to the anaerobic cabinet. The cell suspension was transferred to O-ring sealed centrifuge tubes (Nalgene) and centrifuged outside of the cabinet at 40,000 × g for 45 min at 1 °C.

The supernatant was passed through a HiTrap IMAC HP (1 x 5mL; GE Healthcare) column using an ÄKTA Prime system at 1 mL/min. The column was washed with Buffer A until $A_{280\ nm}$ <0.1. Bound proteins were eluted using a 100 mL linear gradient from 0 to 100% Buffer B (50 mM TRIS, 100 mM $CaCl_2$, 200mM L- Cysteine, 5% glycerol, pH 8). A HiTrap Heparin (1 x 1mL; GE Healthcare) column was used to remove the L- Cysteine, using buffer C (50 mM TRIS, 2 M NaCl, 5% glycerol, pH 8) to elute the protein. Fractions containing RsrR-His were pooled and stored in an anaerobic freezer until needed. RsrR-His protein concentrations were determined using the method of Bradford (Bio-Rad Laboratories) (46), with BSA as the standard. Cluster concentrations were determined by iron assay (47), from which an extinction coefficient, ε, at 455 nm was determined as 3450 ±25 M-1 cm-1, consistent with values reported for [2Fe-2S] clusters with His coordination (23).

Preparation of Apo- RsrR

Apo-RsrR -His was prepared from as isolated holoprotein by aerobic incubation with 1 mM EDTA overnight.

Spectroscopy and mass spectrometry

UV-visible absorbance measurements were performed using a Jasco V500 spectrometer, and CD spectra were measured with a Jasco J810 spectropolarimeter. EPR measurements were performed at 10 K using a Bruker EMX EPR spectrometer (X-band) equipped with a liquid helium system (Oxford Instruments). Spin concentrations in the protein samples were estimated by double integration of EPR spectra with reference to a 1 mM Cu(II) in 10 mM EDTA standard. For native MS analysis, His-tagged RsrR was exchanged into 250 mM ammonium acetate, pH 8, using PD10 desalting columns (GE Life Sciences), diluted to ~21 µM cluster and infused directly (0.3 mL/h) into the ESI source of a Bruker micrOTOF-QIII mass spectrometer (Bruker Daltonics, Coventry, UK) operating in the positive ion mode. Full mass spectra (*m*/*z* 700–3500) were recorded for 5 min. Spectra were combined, processed using the ESI Compass version 1.3 Maximum Entropy deconvolution routine in Bruker Compass Data analysis version 4.1 (Bruker Daltonik, Bremen, Germany). The mass spectrometer was calibrated with ESI-L low concentration tuning mix in the positive ion mode (Agilent Technologies, San Diego, CA).

Electrophoretic Mobility Shift Assays (EMSAs)

DNA fragments carrying the the intergenic region between *sven1847* and *sven1848 of the S. venezualae* chromosome were PCR amplified using *S. venezualae* genomic DNA with 5' 6-FAM modified primers (Table S4). The PCR products were extracted and purified using a QIAquick gel extraction kit (Qiagen) according to the manufacturer's instructions. Probes

were quantitated using a nanodrop ND2000c. The molecular weights of the double stranded FAM labelled probes were calculated using OligoCalc (48).

Bandshift reactions (20 µl) were carried out on ice in 10 mM Tris, 60 mM KCl, pH 7.52. Briefly, 1 µL of DNA was titrated with varying aliquots of RsrR. 2 µL of loading dye (containing 0.01% (w/v) bromophenol blue), was added and the reaction mixtures were immediately separated at 30 mA on a 5% (w/v) polyacrylamide gel in 1 X TBE (89 mM Tris,89 mM boric acid, 2 mM EDTA), using a Mini Protean III system (Bio-Rad). Gels were visualized (excitation, 488 nm; emission, 530 nm) on a molecular imager FX Pro (Bio-Rad). Polyacrylamide gels were pre-run at 30 mA for X min prior to use. For investigations of $[2Fe\text{-}2S]^{1+}$ RsrR DNA binding, in order to maintain the cluster in the reduced state, 5 mM of sodium dithionite was added to the isolated protein and the running buffer (de-gassed for 50 min prior to running the gel). Analysis by UV-visible spectroscopy confirmed that the cluster remained reduced under these conditions.

Funding information. We are grateful to the Natural Environment Research Council for a PhD studentship to John Munnoch, to the Biotechnology and Biological Sciences Research Council for the award of grant BB/J003247/1 (to NLB and MIH), to the UEA Science Faculty for a PhD studentship to Maria Teresa Pellicer Martinez. The funders had no role in study design, data collection and interpretation, or the decision to submit the work for publication.

Acknowledgements. We are grateful to Dr Govind Chandra at the John Innes Centre for advice about ChIP- and dRNA-seq data analysis and to UEA for supporting the mass spectrometry facility. The research presented in this paper was carried out on the High

Performance Computing Cluster supported by the Research and Specialist Computing Support service at the University of East Anglia.

Acknowledgements. We are grateful to Dr Govind Chandra at the John Innes Centre for advice about ChIP- and dRNA-seq data analysis. The research presented in this paper was carried out on the High Performance Computing Cluster supported by the Research and Specialist Computing Support service at the University of East Anglia.

References

1. **Newman DJ**, **Cragg GM**. 2012. Natural products as sources of new drugs over the 30 years from 1981 to 2010. J Nat Prod **75**:311–335.
2. **Challis GL**, **Hopwood D a**. 2003. Synergy and contingency as driving forces for the evolution of multiple secondary metabolite production by Streptomyces species. Proc Natl Acad Sci U S A **100 Suppl** :14555–14561.
3. **Glazebrook M a**, **Doull JL**, **Stuttard C**, **Vining LC**. 1990. Sporulation of Streptomyces venezuelae in submerged cultures. J Gen Microbiol **136**:581–8.
4. **Pullan ST**, **Chandra G**, **Bibb MJ**, **Merrick M**. 2011. Genome-wide analysis of the role of GlnR in Streptomyces venezuelae provides new insights into global nitrogen regulation in actinomycetes. BMC Genomics **12**:175.
5. **Flärdh K**, **Buttner MJ**. 2009. Streptomyces morphogenetics: dissecting differentiation in a filamentous bacterium. Nat Rev Microbiol **7**:36–49.
6. **Rodríguez H**, **Rico S**, **Díaz M**, **Santamaría RI**. 2013. Two-component systems in Streptomyces: key regulators of antibiotic complex pathways. Microb Cell Fact **12**:127.

7. **van Keulen G**, **Alderson J**, **White J**, **Sawers RG**. 2007. The obligate aerobic actinomycete Streptomyces coelicolor A3(2) survives extended periods of anaerobic stress. Environ Microbiol **9**:3143–9.

8. **Johnson EG**, **Sparks JP**, **Dzikovski B**, **Crane BR**, **Gibson DM**, **Loria R**. 2008. Plant-pathogenic Streptomyces species produce nitric oxide synthase-derived nitric oxide in response to host signals. Chem Biol **15**:43–50.

9. **Sasaki Y**, **Oguchi H**, **Kobayashi T**, **Kusama S**, **Sugiura R**, **Moriya K**, **Hirata T**, **Yukioka Y**, **Takaya N**, **Yajima S**, **Ito S**, **Okada K**, **Ohsawa K**, **Ikeda H**, **Takano H**, **Ueda K**, **Shoun H**. 2016. Nitrogen oxide cycle regulates nitric oxide levels and bacterial cell signaling. Sci Rep **6**:22038.

10. **Crack JC**, **Svistunenko DA**, **Munnoch J**, **Thomson AJ**, **Hutchings MI**, **Le Brun NE**. 2016. Differentiated, promoter-specific response of [4Fe-4S] NsrR DNA-binding to reaction with nitric oxide. J Biol Chem jbc.M115.693192.

11. **Crack J**, **Munnoch J**, **Dodd E**, **Knowles F**, **Al Bassam M**, **Kamali S**, **Holland A**, **Cramer S**, **Hamilton C**, **Johnson M**, **Thomson A**, **Hutchings M**, **Le Brun N**. 2015. NsrR from Streptomyces coelicolor is a Nitric Oxide-Sensing [4Fe-4S] Cluster Protein with a Specialized Regulatory Function. J Biol Chem **290**:12689–12704.

12. **Gardner PR**, **Gardner AM**, **Brashear WT**, **Suzuki T**, **Hvitved AN**, **Setchell KDR**, **Olson JS**. 2006. Hemoglobins dioxygenate nitric oxide with high fidelity. J Inorg Biochem **100**:542–550.

13. **Poole RK**, **Hughes MN**. 2000. New functions for the ancient globin family: Bacterial responses to nitric oxide and nitrosative stress. Mol Microbiol **36**:775–783.

14. **Forrester MT**, **Foster MW**. 2012. Protection from nitrosative stress: a central role for microbial flavohemoglobin. Free Radic Biol Med **52**:1620–33.

15. **Hibbing ME**, **Fuqua C**. 2011. Antiparallel and interlinked control of cellular iron

levels by the Irr and RirA regulators of Agrobacterium tumefaciens. J Bacteriol **193**:3461–3472.

16. **Santos J a.**, **Pereira PJB**, **Macedo-Ribeiro S**. 2015. What a difference a cluster makes: The multifaceted roles of IscR in gene regulation and DNA recognition. Biochim Biophys Acta - Proteins Proteomics 1–12.

17. **Nicol JW**, **Helt GA**, **Blanchard SG**, **Raja A**, **Loraine AE**. 2009. The Integrated Genome Browser: Free software for distribution and exploration of genome-scale datasets. Bioinformatics **25**:2730–2731.

18. **Bailey TL**, **Boden M**, **Buske F a**, **Frith M**, **Grant CE**, **Clementi L**, **Ren J**, **Li WW**, **Noble WS**. 2009. MEME SUITE: tools for motif discovery and searching. Nucleic Acids Res **37**:W202–8.

19. **Brekasis D**, **Paget MSB**. 2003. A novel sensor of NADH / NAD + redox poise in Streptomyces coelicolor A3 (2). EMBO J **22**.

20. **Branchu P**, **Matrat S**, **Vareille M**, **Garrivier A**, **Durand A**, **Crépin S**, **Harel J**, **Jubelin G**, **Gobert AP**. 2014. NsrR, GadE, and GadX Interplay in Repressing Expression of the Escherichia coli O157:H7 LEE Pathogenicity Island in Response to Nitric Oxide. PLoS Pathog **10**.

21. **Chhabra S**, **Spiro S**. 2015. Inefficient translation of nsrR constrains behavior of the NsrR regulon in Escherichia coli. Microbiology.

22. **Partridge JD**, **Bodenmiller DM**, **Humphrys MS**, **Spiro S**. 2009. NsrR targets in the Escherichia coli genome: New insights into DNA sequence requirements for binding and a role for NsrR in the regulation of motility. Mol Microbiol **73**:680–694.

23. **Kimura S**, **Kikuchi A**, **Senda T**, **Shiro Y**, **Fukuda M**. 2005. Tolerance of the Rieske-type [2Fe-2S] cluster in recombinant ferredoxin BphA3 from Pseudomonas sp. KKS102 to histidine ligand mutations. Biochem J **388**:869–78.

24. **Lin J**, **Zhou T**, **Ye K**, **Wang J**. 2007. Crystal structure of human mitoNEET reveals distinct groups of iron sulfur proteins. Proc Natl Acad Sci U S A **104**:14640–14645.

25. **Stephens PJ**, **Thomson a J**, **Dunn JB**, **Keiderling T a**, **Rawlings J**, **Rao KK**, **Hall DO**. 1978. Circular dichroism and magnetic circular dichroism of iron-sulfur proteins. Biochemistry **17**:4770–4778.

26. **Link TA**, **Hatzfeld OM**, **Unalkat P**, **Shergill JK**, **Cammack R**, **Mason JR**. 1996. Comparison of the “Rieske” [2Fe-2S] center in the bc1 complex and in bacterial dioxygenases by circular dichroism spectroscopy and cyclic voltammetry. Biochemistry **35**:7546–7552.

27. **Couture MMJ**, **Colbert CL**, **Babini E**, **Rosell FI**, **Mauk AG**, **Bolin JT**, **Eltis LD**. 2001. Characterization of BphF, a Rieske-type ferredoxin with a low reduction potential. Biochemistry **40**:84–92.

28. **Zhang B**, **Crack JC**, **Subramanian S**, **Green J**, **Thomson AJ**, **Le Brun NE**, **Johnson MK**. 2012. Reversible cycling between cysteine persulfide-ligated [2Fe-2S] and cysteine-ligated [4Fe-4S] clusters in the FNR regulatory protein. Proc Natl Acad Sci.

29. **Lee K-L**, **Singh AK**, **Heo L**, **Seok C**, **Roe J-H**. 2015. Factors affecting redox potential and differential sensitivity of SoxR to redox-active compounds. Mol Microbiol n/a–n/a.

30. **Lamb HK**, **Leslie K**, **Dodds AL**, **Nutley M**, **Cooper A**, **Johnson C**, **Thompson P**, **Stammers DK**, **Hawkins AR**. 2003. The negative transcriptional regulator NmrA discriminates between oxidized and reduced dinucleotides. J Biol Chem **278**:32107–32114.

31. **Mishra S**, **Imlay J**. 2012. Why do bacteria use so many enzymes to scavenge hydrogen peroxide? Arch Biochem Biophys **525**:145–160.

32. **Youn HD**, **Kim EJ**, **Roe JH**, **Hah YC**, **Kang SO**. 1996. A novel nickel-containing superoxide dismutase from Streptomyces spp. Biochem J **318 (Pt 3**:889–896.

33. **Hahn J**, **Oh S**, **Roe J**. 2002. Role of OxyR as a peroxide-sensing positive regulator in *Streptomyces coelicolor* A3(2). J Bacteriol **184**:5214–5222.

34. **Kim M-S**, **Dufour YS**, **Yoo JS**, **Cho Y-B**, **Park J-H**, **Nam G-B**, **Kim HM**, **Lee K-L**, **Donohue TJ**, **Roe J-H**. 2012. Conservation of thiol-oxidative stress responses regulated by SigR orthologues in actinomycetes. Mol Microbiol **85**:326–44.

35. **Oh SY**, **Shin JH**, **Roe JH**. 2007. Dual role of OhrR as a repressor and an activator in response to organic hydroperoxides in Streptomyces coelicolor. J Bacteriol **189**:6284–6292.

36. **Shin JH**, **Singh AK**, **Cheon DJ**, **Roe JH**. 2011. Activation of the SoxR regulon in Streptomyces coelicolor by the extracellular form of the pigmented antibiotic actinorhodin. J Bacteriol **193**:75–81.

37. **McLaughlin KJ**, **Strain-Damerell CM**, **Xie K**, **Brekasis D**, **Soares AS**, **Paget MSB**, **Kielkopf CL**. 2010. Structural Basis for NADH/NAD+ Redox Sensing by a Rex Family Repressor. Mol Cell **38**:563–575.

38. **Stuttard C**. 1982. Temperate Phages of Streptomyces venezuelae: Lysogeny and Host Specificity Shown by Phages SV1 and SV2. Microbiology **128**:115–121.

39. **Kieser T**, **Bibb MJ**, **Buttner MJ**, **Chater KF**, **Hopwood DA**. 2000. Practical Streptomyces Genetics. John Innes Cent Ltd 529.

40. **Gust B**, **Challis GL**, **Fowler K**, **Kieser T**, **Chater KF**. 2003. PCR-targeted Streptomyces gene replacement identifies a protein domain needed for biosynthesis of the sesquiterpene soil odor geosmin. Proc Natl Acad Sci U S A **100**:1541–6.

41. **Thompson BJ**, **Widdick D a**, **Hicks MG**, **Chandra G**, **Sutcliffe IC**, **Palmer T**, **Hutchings MI**. 2010. Investigating lipoprotein biogenesis and function in the model

585 Gram-positive bacterium Streptomyces coelicolor. Mol Microbiol **77**:943–957.

586 42. **Hutchings MI**, **Hong H-J**, **Buttner MJ**. 2006. The vancomycin resistance VanRS
587 two-component signal transduction system of Streptomyces coelicolor. Mol Microbiol
588 **59**:923–35.

589 43. **Al-Bassam MM**, **Bibb MJ**, **Bush MJ**, **Chandra G**, **Buttner MJ**. 2014. Response
590 regulator heterodimer formation controls a key stage in Streptomyces development.
591 PLoS Genet **10**:e1004554.

592 44. **Reja R**, **Vinayachandran V**, **Ghosh S**, **Pugh BF**. 2015. Molecular mechanisms of
593 ribosomal protein gene coregulation. Genes Dev **29**:1942–1954.

594 45. **Amman F**, **Wolfinger MT**, **Lorenz R**, **Hofacker IL**, **Stadler PF**, **Findeiß S**. 2014.
595 TSSAR: TSS annotation regime for dRNA-seq data. BMC Bioinformatics **15**:89.

596 46. **Bradford MM**. 1976. A rapid and sensitive method for the quantitation of microgram
597 quantities of protein utilizing the principle of protein-dye binding. Anal Biochem
598 **72**:248–254.

599 47. **Crack J**, **Green J**, **Le Brun N**, **Thomson A**. 2006. Detection of Sulfide Release from
600 the Oxygen-sensing [4Fe-4S] Cluster of FNR. J Biol Chem **281**:18909–18913.

601 48. **Kibbe WA**. 2007. OligoCalc: An online oligonucleotide properties calculator. Nucleic
602 Acids Res **35**:43–46.

603

604

605 **Figure Legends**

606 **Table 1. Combined ChIP-Seq and dRNA-Seq data for selected RsrR targets.**

607 [a] – Genes flanking the ChIP peak.

608 [b] – Distance to the translational start codon (bp).

609 [c] – Distance to the transcriptional start site (bp).

610 [d] – Fold change WT vs.Mutant, values normalised per million reads per sample

611 [e] – EMSA shift reactions have been carried out successfully and specifically

612 [f] – A fold change <-2 or >2

613 _ - Class 1 targets.

614

615 **FIG. 1. Defining the regulon and binding site for RsrR.** Top panel (A) shows the whole
616 genome ChIP-seq analysis with class 1 sites labelled in black. The frequency of each base
617 sequenced is plotted with genomic position on the x-axis and frequency of each base
618 sequenced on the y-axis for *S. venezualae* (NC_018750). Bottom panel (B) shows the class 1
619 and 2 web logos generated following MEME analysis of the ChIP-seq data.

620

621 **FIG 2. Spectroscopic characterization of RsrR.** UV-visible absorption **(A**), CD (**B**) and
622 EPR spectra (**C**) of 309 µM [2Fe-2S] RsrR (~75% cluster-loaded). Black lines – as isolated,
623 red lines – oxidised, grey lines reduced proteins. In A and B, initial exposure to ambient O_2
624 for 30 min was followed by 309 µM sodium dithionite treatment; in C – as isolated protein
625 was first anaerobically reduced by 309 µM sodium dithionite and then exposed to ambient O_2
626 for 50 min. A 1 mm pathlength cuvette was used for optical measurements. Inset in (A)
627 shows details of the iron-sulfur cluster absorbance in the 300 – 700 nm region.

628 **FIG 3. Native mass spectrometry of RsrR.** (**A**) and (**B**) Positive ion mode ESI-TOF native
629 mass spectrum of ~21 µM [2Fe-2S] RsrR in 250 mM ammonium acetate pH 8.0, in the RsrR
630 monomer (A) and dimer (B) regions. Full *m*/*z* spectra were deconvoluted with Bruker
631 Compass Data analysis with the Maximum Entropy plugin.

632

633 **FIG 4. Cluster- and oxidation state-dependent DNA binding by [2Fe-2S] RsrR.** EMSAs
634 showing DNA probes unbound (U), bound (B), and non-specifically bound (NS) by (**A**) [2Fe-

635 2S]$^{2+}$ and apo-RsrR, (**B**) [2Fe-2S]$^{2+}$ RsrR and (**C**) [2Fe-2S]$^{1+}$ RsrR. Ratios of [2Fe-2S] RsrR
636 and [RsrR] to DNA are indicated. DNA concentration was 3.5 nM for the [2Fe-2S] $^{2+/1+}$ and
637 apo-RsrR experiments. For (A) and (B) the reaction mixtures were separated at 30 mA for 50
638 min and the polyacrylamide gels were pre-run at 30 mA for 2 min prior to use. For (C) the
639 reaction mixtures were separated at 30 mA for 1h 45 min and the polyacrylamide gel was
640 pre-run at 30 mA for 50 min prior to use using the de-gassed running buffer containing 5 mM
641 sodium dithionite.
642
643 **FIG 5. Oxidised RsrR binding to full site (class 1) and half site (class 2) RsrR targets**.
644 EMSAs showing DNA probes unbound (U) and bound (B) by [2Fe-2S]$^{2+}$. Ratios of [2Fe-2S]
645 RsrR and [RsrR] to DNA are indicated. DNA concentration was 20 nM for each probe.
646 EMSA's using class 2 promoters *sven0247* and *sven0519* (A), class 1 probes from the RsrR
647 *rsrR* binding region (B) and the four possible half sites from the *rsrR* class 1 sites (C) were
648 used. For (A) the reaction mixtures were separated at 30 mA for 1h and the polyacrylamide
649 gel was pre-run at 30 mA for 2 min prior to use. For (B) and (C) the reaction mixtures were
650 separated at 30 mA for 30 min and the polyacrylamide gels were pre-run at 30 mA for 2 min
651 prior to use.
652
653 **FIG 6. Graphical representation of combined ChIP-Seq, ChIP-exo and dRNA-seq for**
654 **four class 1 targets.** Each target has the relative position of ChIP-exo (blue line) peak centre
655 (dotted line) and putative transcriptional start site (TSS - solid arrow) indicated with the
656 distance in bp (black numbers) relative to the down stream start codon of target genes. The y-
657 axis scale corresponds to number of reads for ChIP data with each window corresponding to
658 200 bp with each ChIP-peak being ~50 bp wide. Above each is the relative binding site

659 sequence coloured following the weblogo scheme (A – red, T – green, C – blue and G –
660 yellow) from the MEME results.
661
662 **Supplementary FIG S1. Sven6563 is not an NsrR homologue.** Top panal, alignment of *S.*
663 *coelicolor* NsrR (ScNsrR) with the annotated NsrR protein in *S. venezuelae* (Sven6563)
664 reveals only 27% amino acid identity. Bottom panal, *Streptomyces* NsrR proteins are
665 genetically linked to genes encoding the NO dioxygenase HmpA, e.g. shown here in *S.*
666 *coelicolor* where ScNsrR regulates itself and both HmpA homologues and is linked to *hmpA1*.
667 ScNsrR binding sites are shown as orange boxes. *S. venezuelae* does not encode an HmpA
668 homologue and Sven6563 is divergently transcribed from *sven6562* which encodes a LysR
669 family regulator with an NmrA-type NAD/NADP binding domain. NmrA (PMID: 12764138)
670 is a transcriptional repressor in fungi which can distinguish between oxidised and reduced
671 NAD and NADP and may be a redox sensor. Both *sven6562* and *sven6563* are repressed by
672 Sven6563 binding to two adjoining 25 bp sites.
673
674 **Supplementary FIG S2. RsrR homologues from DELTA BLASTP.** Alignment of *S.*
675 *venezuelae* Sven6563 (RsrR) with the top hits from a DELTA BLASTP search, all have
676 >70% identity and all are in filamentous actinomycetes. The other hits in the top 100 were all
677 IscR proteins from proteobacteria with 25-27% identity to RsrR. The three cysteine residues
678 that most likely ligate the cluster are boxed.
679
680 **Supplementary data File S3.1 – S3.2.** Contained within this excel sheet are the tab-
681 delimited results of ChIP-seq and dRNA-seq results wt vs *rsrR::apr of S. venzualae* (16 hour
682 time point). ChIP-seq (cut offs of >0, (S3.1) >200 (S3.2) and >500 reads (S3.3) - combined
683 and standalone ChIP data (S3.4) and dRNA-seq (both gene expression results (S3.5) and

TSSAR defined Transcriptional start sites (for WT +ve strand (S3.6), WT -ve strand (S3.7), mutant +ve stran (S3.8 and Mutant -ve strand (S3.9). Columns A-D - ChIP-seq analysis was carried out using the default setting of CLC workbench 8 producing. Columns E-O - produced by taking the closest Transcriptional start codon upstream (5' end) of the ChIP-peak and P-Y by taking the closes Transcriptional start codon downstream (3'' end) from the ChIP-peak. Column F and Q - The location of the 5' Start codon. Column G and R - The location of the associate 5' TSS. Column H and S - the number of bases from the ChIP-peak centre to the gene (this value is independent of orientation so the peak maybe at the 3' end of the gene ultimately indicating why numbers may be in the thousands). (e.g. column B - H or B - S). Column I and T - the number of bases from the ChIP-peak centre to the TSS. (e.g. column B - I or B - T). Column J and U - The TSS class as defined by TSSAR in this sheet only P was retained standing for primary TSS (within 250 bp of the gene start site upstream 5'-3'). Column K and V - The TSSAR comment indicating where the TSS is in regards to its gene. Column L and W - The RNA-seq Fold change of WT vs mutant (*rsrR::apr*). Column M and X - Regulation type of the WT vs Mutant (up regulated indicating that expression is higher in the mutant background). Column N and Y - The gene annotation for each target from the NC_018750.1.ptt file.

Supplementary data File S3.3. Contained within this excel sheet are the tab-delimited results of ChIP-seq and dRNA-seq results wt vs *rsrR::apr of S. venezualae* ChIP-seq (cut offs of >500 reads (3.3) - combined dRNA-seq expression results and TSSAR defined Transcriptional start sites (for WT +ve strand, WT -ve strand, mutant +ve strand Mutant -ve strand. Column A - gene numbers identified by taking the most likely associate gene (e.g. closest gene, downstream of the binding sequence). Column B - The location of the 5' Start codon. Column C - The location of the associate 5' TSS. Column D - the number of bases

709 from the ChIP-peak centre to the gene (this value is independent of orientation so the peak
710 maybe at the 3' end of the gene ultimately indicating why numbers may be in the thousands).
711 Column E - the number of bases from the ChIP-peak centre to the TSS. Column F - The TSS
712 class as defined by TSSAR in this sheet only P was retained standing for primary TSS
713 (within 250 bp of the gene start site upstream 5'-3'). Column G - The TSSAR comment
714 indicating where the TSS is in regards to its gene. Column H - The RNA-seq Fold change of
715 WT vs mutant (*rsrR::apr*). Column I - Regulation type of the WT vs Mutant (up regulated
716 indicating that expression is higher in the mutant background). Column J - The gene
717 annotation for each target from the NC_018750.1.ptt file.
718
719 **Supplementary data File 3.4.** CLC workbench 8 results of WT *S. venezualae* vs mutant
720 (*rsrR::apr pMs82 3xFlag rsrR*). Columns A - The called peak region. Column B - The left
721 edge of the peak. Column C - The right edge of the peak. Column D - The centre of the peak.
722 Column E - The width of the peak (C-B)
723
724 **Supplementary data File 3.5.** Contained in this sheet are the RNA-seq expression results of
725 WT and RsrR mutant using the default setting of CLC workbench 8. Column A -
726 *Streptomyces venezualae* gene number (from genome NC_018750.1). Columns B-F -
727 Experimental results of WT vs. Mutant. Column G-L - WT expression results. Column M-R -
728 *rsrR::apr* (mutant) expression results. Normalisation was carried out per million reads
729 mapped.
730
731 **Supplementary data File 3.6.** Contained in this sheet are the dRNA-seq transcriptional start
732 site (TSS) identification results (WT +ve strand) from the TSSAR webservice
733 (http://nibiru.tbi.univie.ac.at/TSSAR/) - doi:10.1186/1471-2105-15-89 Settings: p-value =

1e-4, noise threshold = 2 and merge range = 5 (with a 1000 bp window). Column A - *Streptomyces venezualae* gene number (from genome NC_018750.1). Columns B-F - Experimental results of WT vs. Mutant. Column G-L - WT expression results. Column M-R - *rsrR::apr* (mutant) expression results. Normalisation was carried out per million reads mapped.

Supplementary data File 3.7. Contained in this sheet are the dRNA-seq transcriptional start site (TSS) identification results (WT -ve strand) from the TSSAR webservice (http://nibiru.tbi.univie.ac.at/TSSAR/) - doi:10.1186/1471-2105-15-89 Settings: p-value = 1e-4, noise threshold = 2 and merge range = 5 (with a 1000 bp window). Column A - *Streptomyces venezualae* gene number (from genome NC_018750.1). Columns B-F - Experimental results of WT vs. Mutant. Column G-L - WT expression results. Column M-R - *rsrR::apr* (mutant) expression results. Normalisation was carried out per million reads mapped.

Supplementary data File 3.8. Contained in this sheet are the dRNA-seq transcriptional start site (TSS) identification results (*rsrR::apr* +ve strand) from the TSSAR webservice (http://nibiru.tbi.univie.ac.at/TSSAR/) - doi:10.1186/1471-2105-15-89 Settings: p-value = 1e-4, noise threshold = 2 and merge range = 5 (with a 1000 bp window). Column A - *Streptomyces venezualae* gene number (from genome NC_018750.1). Columns B-F - Experimental results of WT vs. Mutant. Column G-L - WT expression results. Column M-R - *rsrR::apr* (mutant) expression results. Normalisation was carried out per million reads mapped.

Supplementary data File 3.9. Contained in this sheet are the dRNA-seq transcriptional start site (TSS) identification results (*rsrR::apr* +ve strand) from the TSSAR webservice

(http://nibiru.tbi.univie.ac.at/TSSAR/) - doi:10.1186/1471-2105-15-89 Settings: p-value = 1e-4, noise threshold = 2 and merge range = 5 (with a 1000 bp window). Column A - *Streptomyces venezualae* gene number (from genome NC_018750.1). Columns B-F - Experimental results of WT vs. Mutant. Column G-L - WT expression results. Column M-R - *rsrR::apr* (mutant) expression results. Normalisation was carried out per million reads mapped.

Supplementary data File 3.10. Contained in this sheet are the combined ChIP-seq/exo and dRNA-seq transcriptional start site (TSS) identification results from the TSSAR webservice (http://nibiru.tbi.univie.ac.at/TSSAR/) - doi:10.1186/1471-2105-15-89. Shown specifically are the Exo peaks that have reported TSS informaiton from the 16h time point. Settings for TSSAR: p-value = 1e-4, noise threshold = 2 and merge range = 5 (with a 1000 bp window). Column A - *Strptomyces venezualae* gene number (from genome NC_018750.1). Columns B-F - Experimental results of WT vs. Mutant

Column G-L - WT expression results. Column M-R - *rsrR::apr* (mutant) expression results. Normalisation was carried out per million reads mapped.

Supplementary data File S4. Contained in this file is the class 2 identified MEME binding site information. This is the raw output of the MEME analysis and includes all MEME output results.

Supplementary data File S5. Contained in this file is the class 1 identified MEME binding site information. This is the raw output of the MEME analysis and includes all MEME output results.

Supplementary Fig. S6. Full range native mass spectrum of RsrR. Positive ion mode ESI-TOF native mass spectrum of ~21 μM [2Fe-2S] RsrR in 250 mM ammonium acetate pH 8.0, The full *m*/*z* spectrum was deconvoluted with Bruker Compass Data analysis with the Maximum Entropy plugin.

Supplementary Table S7. Strains and plasmids used during this study.

Supplementary Table S8. List of primers used in this study. Primers JM0119-JM0134 were used to produce EMSA DNA templates that were successfully shifted using purified RsrR and mentioned in the text but the data is not shown as part of the work.

Table 1. Combined ChIP-Seq and RNA-Seq data for selected RsrR targets.

Flanking gene[a]					
Left (-1)	Right (+1)	Distance[b]	Dist. TSS[c]	Fold Change[d]	Annotation
	sven0372[e]	-2328	-2443	-1.15	Putative two-component system sensory histidine kinase
	sven0519[e]	-993		1.59	Sulfate permease
	sven0772	-408		-1.96	NAD- or NADP-dependent oxidoreductases
sven0903		1440	1406	1.06	Uracil DNA glycosylase superfamily
	sven1377	29		1.08	DeoR family Transciptional regulator, HTH domain WYL domain.
sven1490		192	192	2.72[f]	Alpha/beta hydrolase family
	sven1561[e]	103	67	1.02	Amidohydrolase
	sven1670	17		-1.2	Pyridoxamine 5'-phosphate oxidase
sven1685		1215		1.18	CoA-transferase family III
	sven1847[e]	6		-1.83	The short-chain dehydrogenases/reductases family (SDR)[2] known to be NAD- or NADP-dependent oxidoreductases
	sven1902	-1643	-1689	1.02	Glutamate-ammonia ligase adenylyltransferase, GlnD PII-uridylyltransferase
	sven2177	-397	-440	1.31	citrate lyase beta subunit, C-C_Bond_Lyase of the TIM-Barrel fold
	sven2494	91	91	-1.82	insignificant results showing Transposase/zinc ribbon fragments
	sven2540	221		-1.9	Oxidoreductase family, NAD-binding Rossmann fold
sven2680	*sven2681*	-80, -416	-146, -374	-1.12,-69.97[f]	ATP or GTP-binding protein, Protease inhibitorDrug resistance transporter, EmrB or QacA family, major fascilitator family domain
sven2931	*sven2932*	48, -103		-2.43[f], 6.48[f]	Esterase A, Beta-lactamase (fragment)
sven3087		2092	2092	1.04	Acetyltransferase (GNAT) domain
	sven3827[e]	-902	36	-1.48	SAICAR synthetase
sven3848	*sven3849*	12, 429		69.33[f], -1.22	ATP-dependent helicase, a large c-terminal domain of unknown functionhypothetical protein
	sven3934	-1228		1.27	Enhanced intracellular survival protein, Sterol carrier protein domain, Acetyltransferase (GNAT) domain
sven3970	*sven3971*	1102, -1647	1139	1.13, -1.38	SpoU rRNA Methylase family, RNA 2'-O ribose methyltransferase substrate bindingDoxX

	sven4022	-772		-1.78	NAD(P)-binding Rossmann-like domain (fragment)
sven4076		375		-1.53	Archaeal seryl-tRNA synthetase-related sequence
sven4272	*sven4273*	1362-573		1.141.33	NADH-ubiquinone oxidoreductase chain H, I and dicluster domain [4Fe-4S]
sven4418		588	589	1.3	Glutamine amidotransferase domain (fragment).
	sven4888	-528		1.8	Glutamate-1-semialdehyde aminotransferase
	sven4955	-602		1.11	PadR-like family transcriptional regulator
	sven5065	-221	-252	1.63	Putative MarR family transcriptional regulator
	sven5088	-77		-1.02	NAD dependent epimerase/dehydratase family
	sven5174[e]	-119		-1.09	Quinone oxidoreductase, Zinc-binding dehydrogenase, Alcohol dehydrogenase GroES-like domain
sven5492	*sven5493*	513, -1899	413, -1899	1.2; -1.16	*sven*5392, Putative ATP-dependent DNA helicase RecQ like,
sven5583	*sven5584*	594, -1463		2.14[f], 2.33[f]	Methylisocitrate lyase, Phosphoenolpyruvate phosphomutase2-methylcitrate synthase, Citrate synthase
sven5665	*sven5666*	634, -876	492	1.01, 2.45[f]	Haloacid dehalogenase-like hydrolase, hypothetical protein
sven5907	*sven5908*	1156, -296	-295	-2.17[f], 1.1	Bacterial extracellular solute-binding protein (Fragment)domains of unknown function
	sven6227	-1279		-15.99[f]	NADH-FMN oxidoreductase
sven6534		3352		1.62	Trypsin-like peptidase domain
sven6562[e]	*sven6563*[e]	72, -35	36	62.98[f],N/A	*nmrA/rsrR*
sven6836		1547		-2.21	FAD binding domain (Succinate/Fumarate reductase flavoprotein C-term)
sven7046	*sven7047*	658, -447	591	1.16, -1.23	Stress-induced transcription regulator, Cobalt transporter subunit (CbtA)
sven7248		538		3.83[f]	FAD dependent oxidoreductase, Rieske [2Fe-2S] domain
sven7284	*sven7285*	-55, -197	-167	1.13, 35.61[f]	Transcriptional regulator PadR-like family, Putative transcriptional regulator
sven7296	*sven7297*	314, -6	137	2.33[f], -1.33	Putative integral membrane protein, tetR family transcriptional regulator

[a] – Genes flanking the ChIP peak.
[b] – Distance to the translational start codon (bp).
[c] – Distance to the transcriptional start site (bp).
[d] – Fold change WT vs.Mutant, values normalised per million reads per sample
[e] – EMSA shift reactions have been carried out successfully and specifically
[f] – A fold change <-2 or >2
- Class 1 targets.

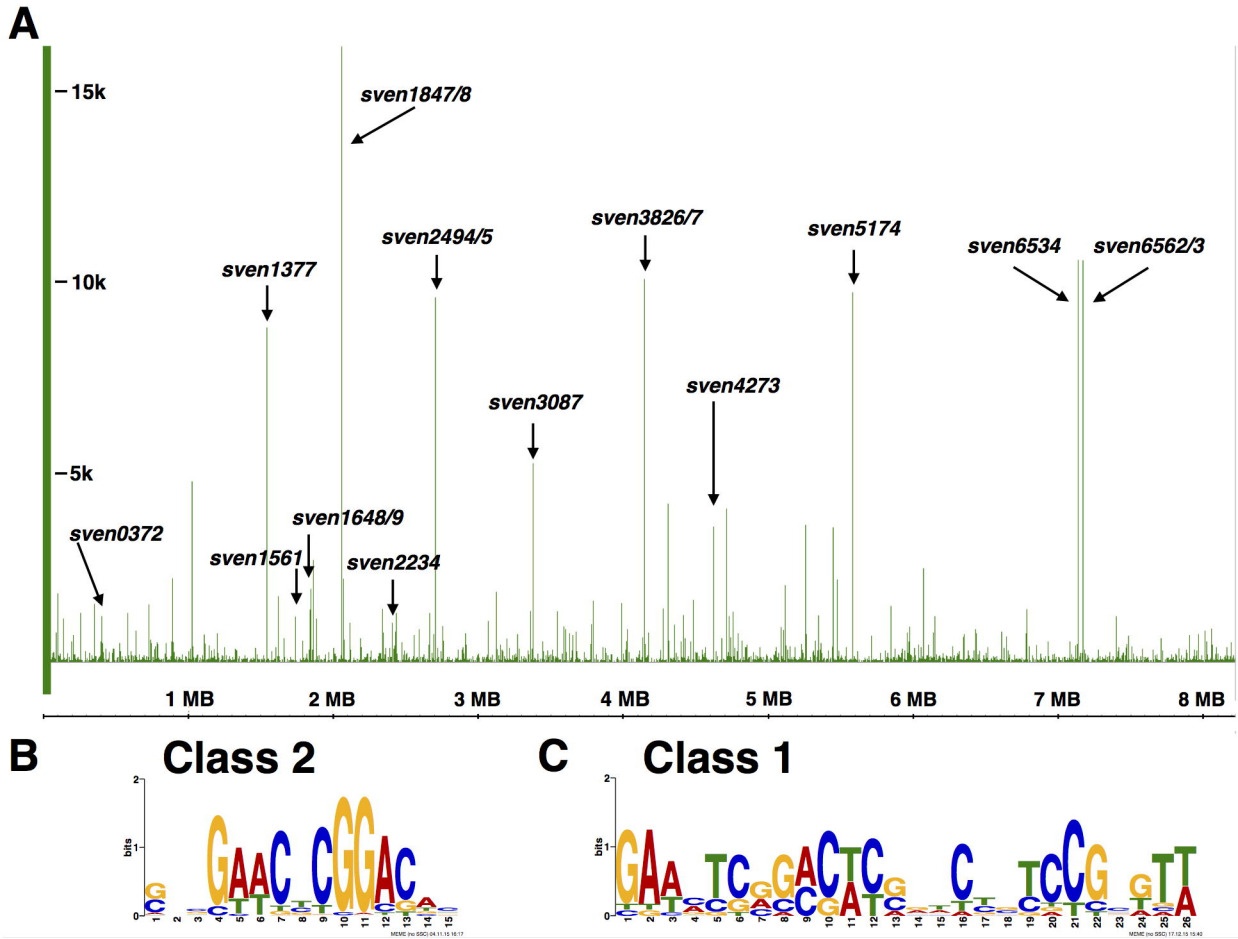
A
15k
10k
5k
sven1847/8
sven1377
sven2494/5
sven3826/7
sven5174
sven6534
sven6562/3
sven3087
sven4273
sven0372
sven1648/9
sven1561
sven2234
1 MB
2 MB
3 MB
4 MB
5 MB
6 MB
7 MB
8 MB
B
Class 2
bits
C
Class 1
bits

A

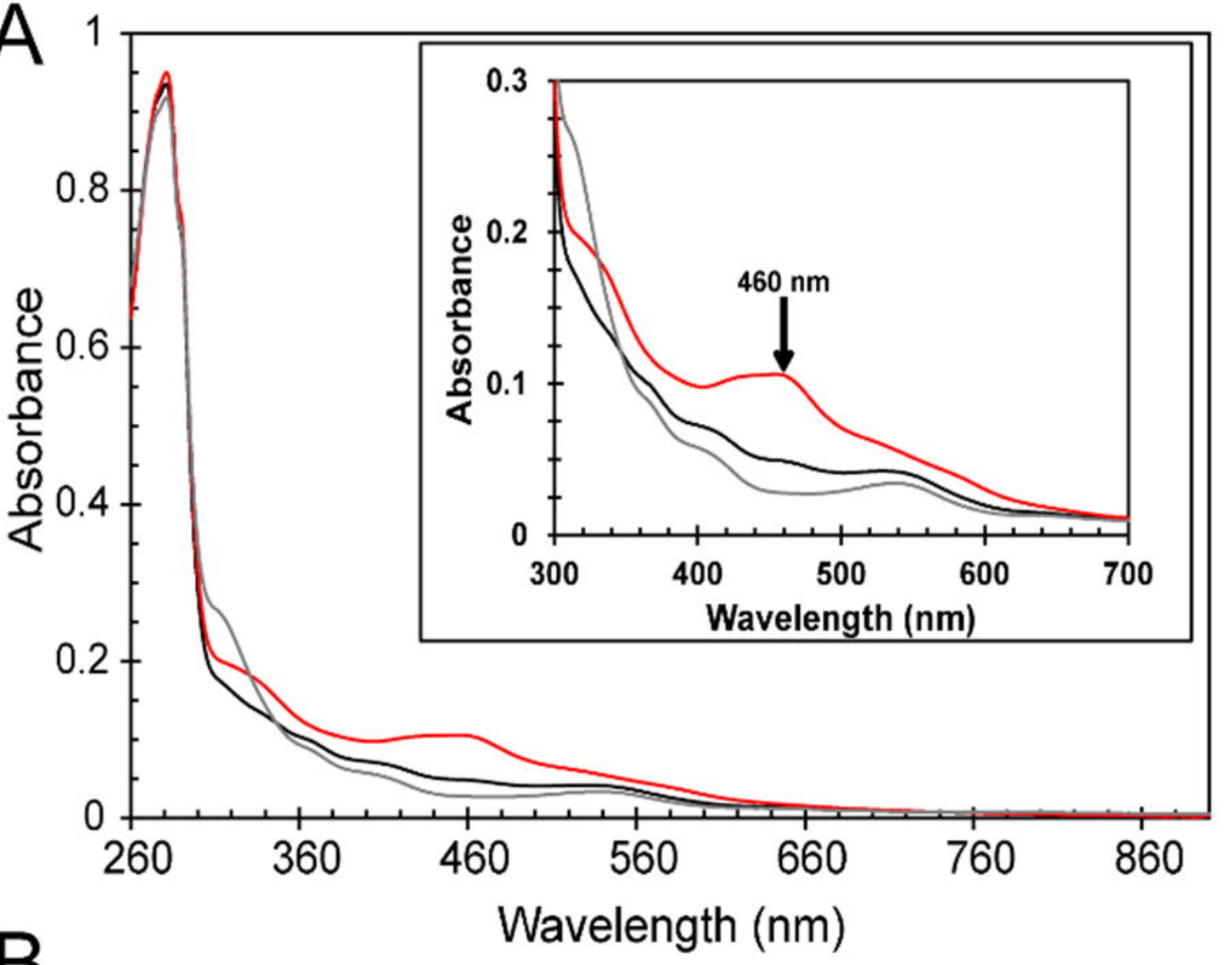

B

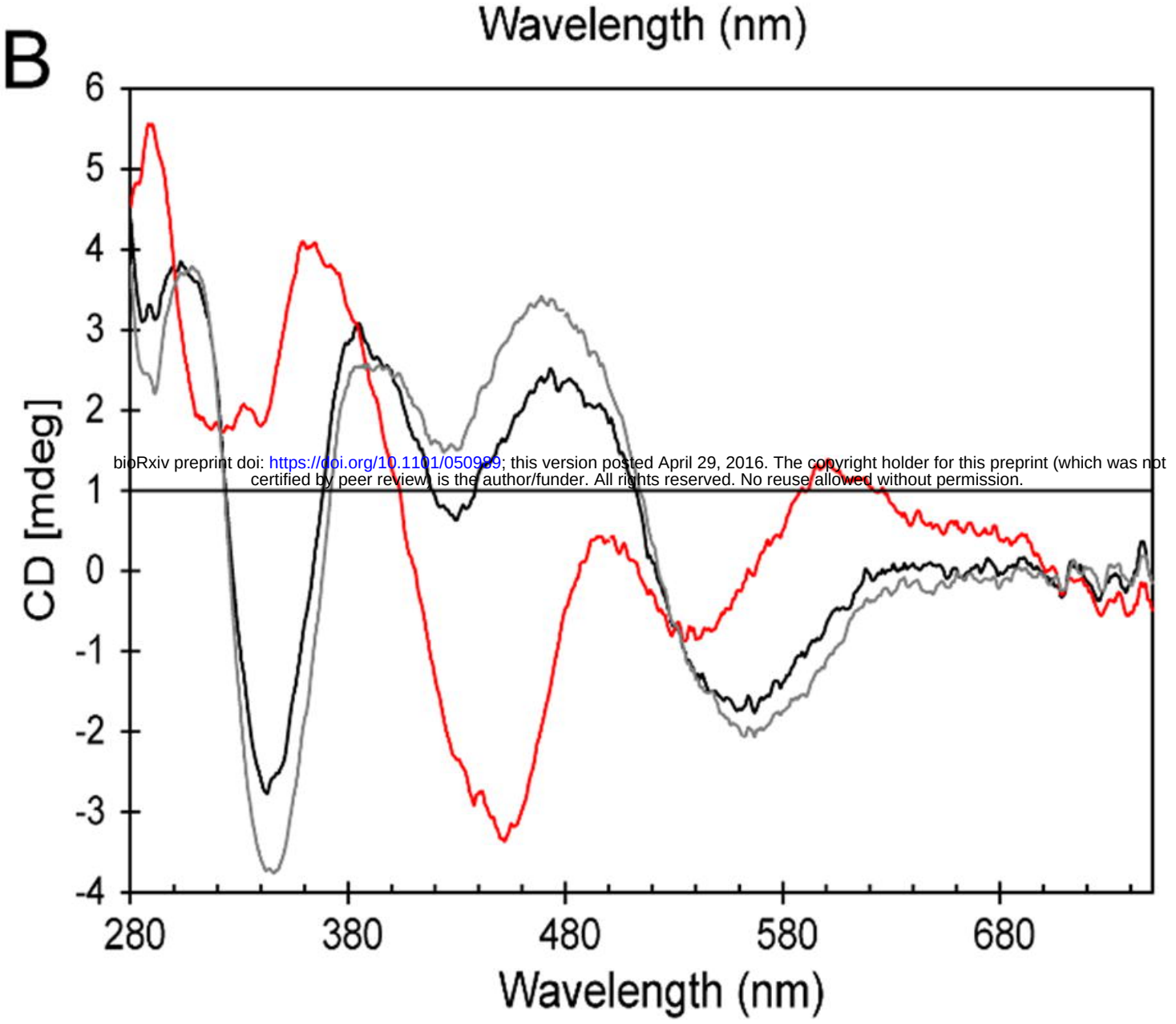

C

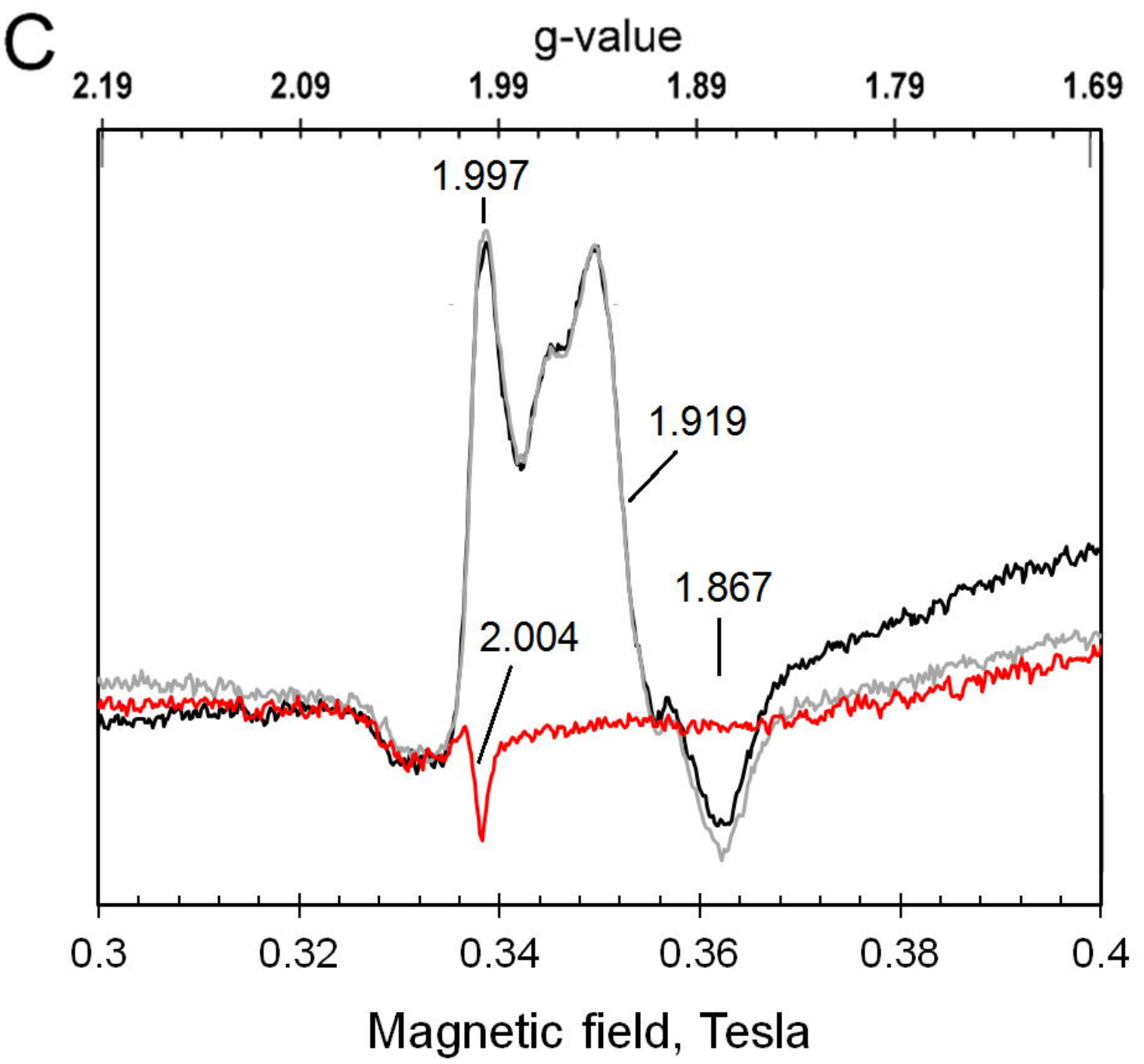

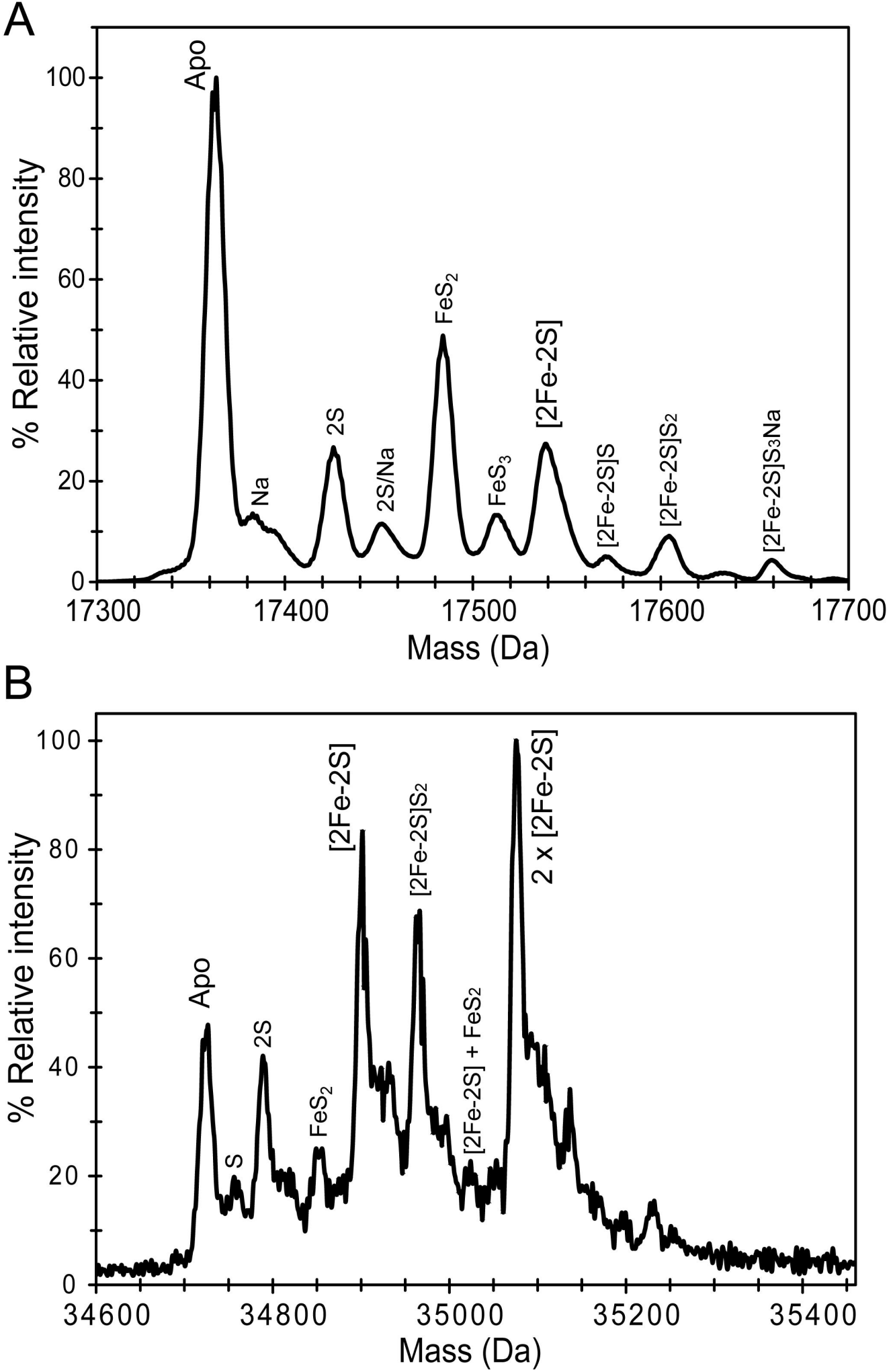
A
Apo
Na
2S
2S/Na
FeS2
FeS3
[2Fe-2S]
[2Fe-2S]S
[2Fe-2S]S2
[2Fe-2S]S3Na
% Relative intensity
Mass (Da)
B
Apo
S
2S
FeS2
[2Fe-2S]
[2Fe-2S]S2
[2Fe-2S] + FeS2
2 x [2Fe-2S]
% Relative intensity
Mass (Da)

A

$[2Fe\text{-}2S]^{2+}$ RsrR (nM)	-	60	100	-	-	-	-
Ratio [Fe-S]:DNA	-	17	29	-	-	-	-
Apo RsrR (nM)	-	88	147	87	105	122	140
Ratio Apo RsrR:DNA	-	25	42	25	30	35	40

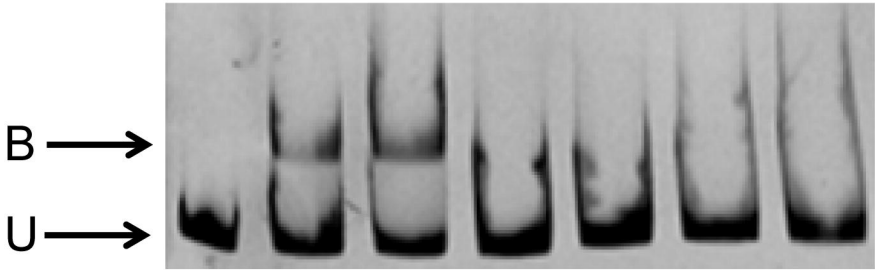

B

$[2Fe\text{-}2S]^{2+}$ RsrR (nM)	-	60	80	100	120	140
Ratio [Fe-S]:DNA	-	17	23	29	34	40

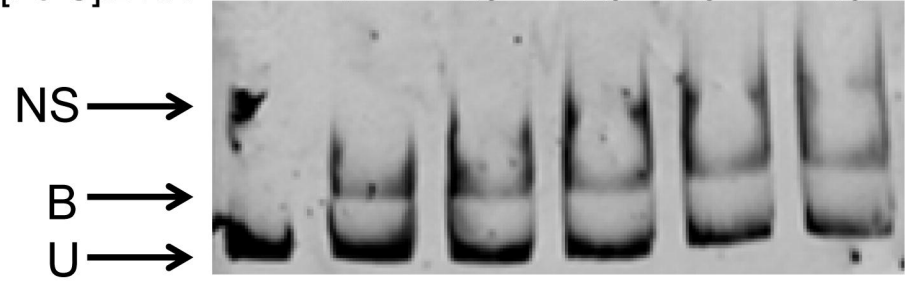

C

$[2Fe\text{-}2S]^{1+}$ RsrR (nM)	-	60	80	100	120	140
Ratio [Fe-S]:DNA	-	17	23	29	34	40

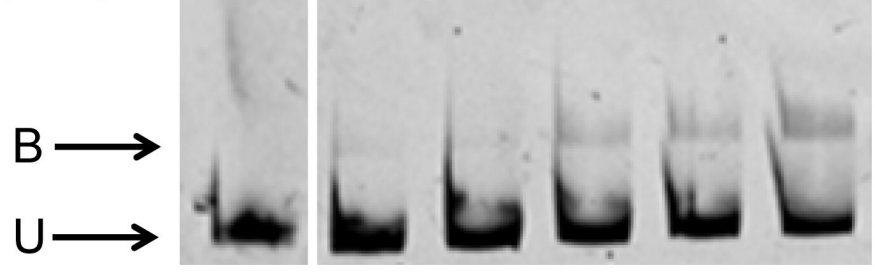

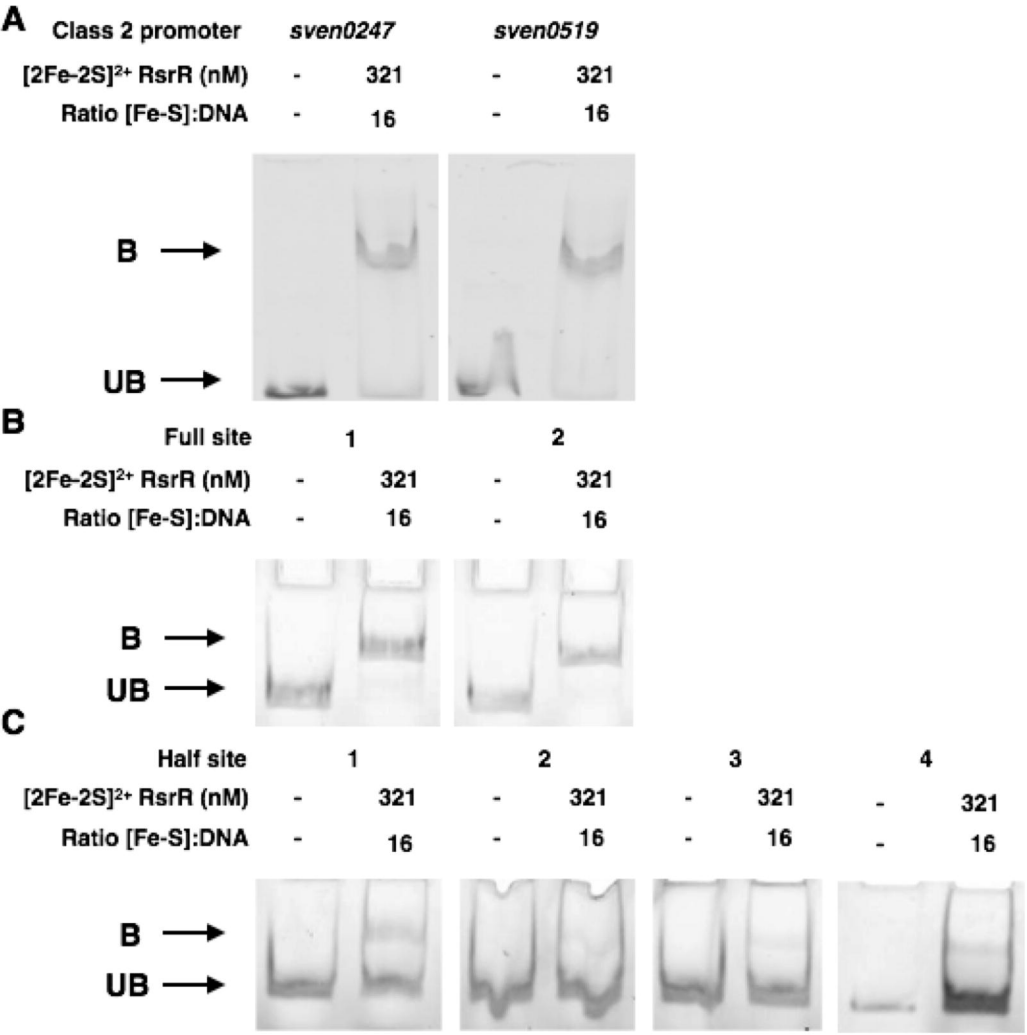
A
Class 2 promoter
sven0247
sven0519
[2Fe-2S]2+ RsrR (nM)
- 321 - 321
Ratio [Fe-S]:DNA
- 16 - 16
B
UB
B
Full site
1
2
[2Fe-2S]2+ RsrR (nM)
- 321 - 321
Ratio [Fe-S]:DNA
- 16 - 16
B
UB
C
Half site
1
2
3
4
[2Fe-2S]2+ RsrR (nM)
- 321 - 321 - 321 - 321
Ratio [Fe-S]:DNA
- 16 - 16 - 16 - 16
B
UB

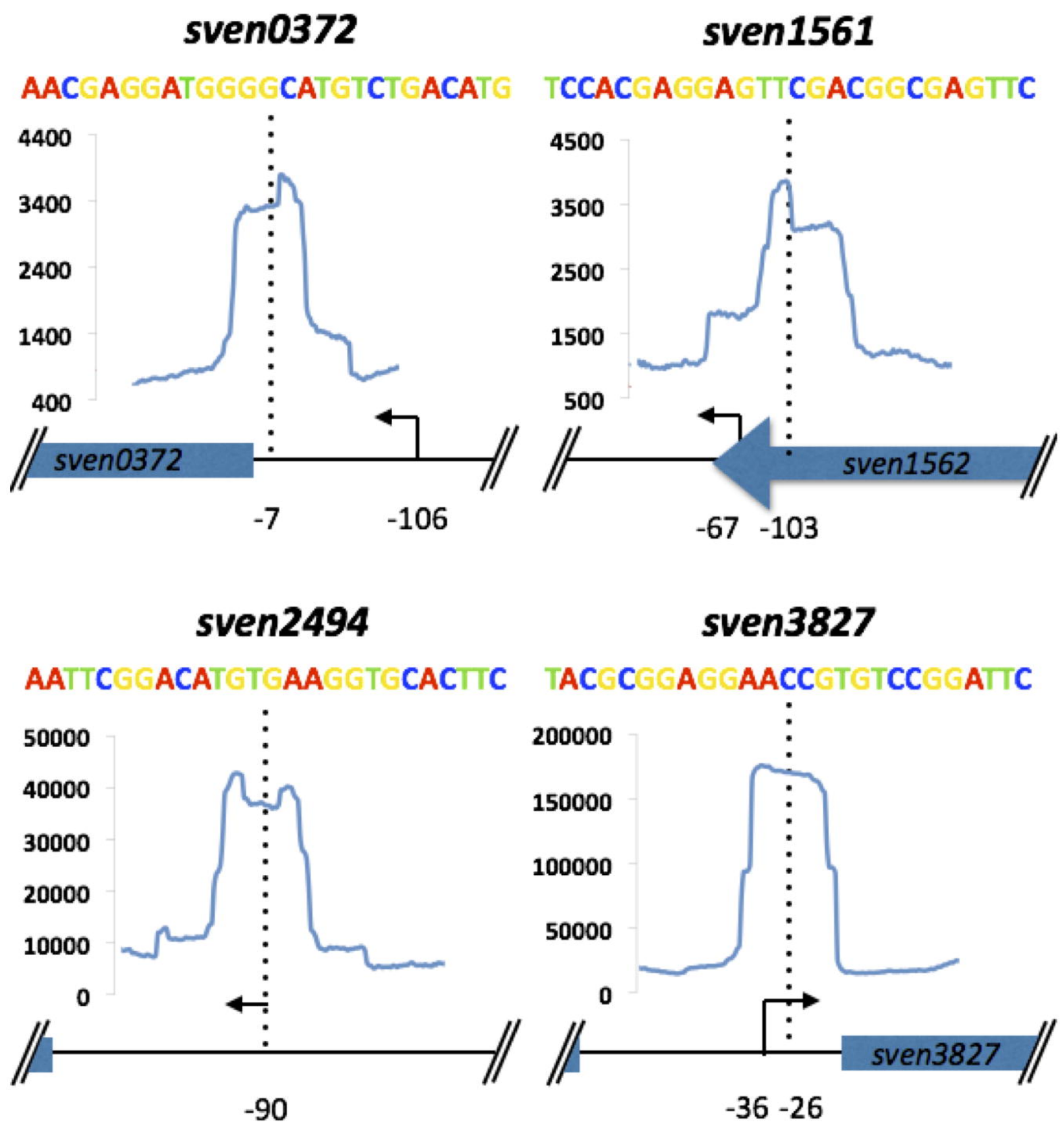
sven0372
AACGAGGATGGGGCATGTCTGACATG
4400
3400
2400
1400
400
sven0372
-7
-106
sven1561
TCCACGAGGAGTTCGACGGCGAGTTC
4500
3500
2500
1500
500
sven1562
-67
-103
sven2494
AATTCGGACATGTGAAGGTGCACTTC
50000
40000
30000
20000
10000
0
-90
sven3827
TACGCGGAGGAACCGTGTCCGGATTC
200000
150000
100000
50000
0
sven3827
-36
-26